

20 **Abstract**

21 Ile-Pro-Pro (IPP) and Leu-Lys-Pro (LKP) are food-derived antihypertensive peptides which
22 inhibit angiotensin-converting enzyme (ACE) and may have potential to attenuate
23 hypertension. There is debate over their mechanism of uptake across small intestinal
24 epithelia, but paracellular and PepT1 carrier-mediated uptake are thought to be important
25 routes. The aim of this study was to determine their routes of intestinal permeability using *in*
26 *vitro*, *ex vivo* and *in vivo* intestinal models. The presence of an apical side pH of 6.5
27 (mimicking the intestinal acidic microclimate) and of Gly-Sar (a high affinity competitive
28 inhibitor and substrate for PepT1) were tested on the transepithelial apical to basolateral (A to
29 B) transport of [³H]-IPP and [³H]-LKP across filter-grown Caco-2 monolayers *in vitro* and rat
30 jejunal mucosae *ex vivo*. A buffer pH of 6.5 on the apical side enabled Gly-Sar to reduce the
31 apparent permeability (P_{app}) of [³H]-IPP and [³H]-LKP, but this inhibition was not evident at
32 an apical buffer pH of 7.4. Gly-Sar reduced the P_{app} across isolated jejunal mucosae and the
33 area under the curve (AUC) in intra-jejunal instillations when the apical/luminal buffer pH
34 was either 7.4 or 6.5. However, the jejunal surface acidic pH was maintained in rat jejunal
35 tissue even when the apical side buffer pH was 7.4 due to the presence of the microclimate
36 which is not present in monolayers. PepT1 expression was confirmed by
37 immunofluorescence on monolayers and brush border of rat jejunal tissue. This data suggest
38 that IPP and LKP are highly permeable and cross small intestinal epithelia in part by the
39 PepT1 transporter, with an additional contribution from the paracellular route.

40

41

42 **Keywords:** Antihypertensive peptides; food-derived bioactives; intestinal transport; PepT1;
43 Ile-Pro-Pro; Leu-Lys-Pro; transport models.

44 **1 Introduction**

45 Food-derived bioactive peptides may provide beneficial physiological effects when released
46 from parent proteins [1]. Recent research has focused on food-derived peptides with potential
47 anti-hypertensive, anti-diabetic, anti-oxidant and anti-inflammatory activities. To date, such
48 peptides have shown modest effects in human trials, and together with the equivocal efficacy,
49 their epithelial permeation pathways across the small intestine are still unknown [2-5]. The
50 antihypertensive lactotripeptide, Ile-Pro-Pro (IPP) was isolated from bovine milk β -casein
51 following fermentation by *Lactobacillus helveticus* [6]. Leu-Lys-Pro (LKP) isolated from the
52 bonito fish muscle also has anti-antihypertensive properties [7]. They are both competitive
53 inhibitors of angiotensin converting enzyme (ACE) albeit with low potency, but nevertheless
54 they induce hypotensive responses in the Spontaneously Hypertensive Rat (SHR) model
55 following either intravenous or oral administration [8, 9].

56

57 IPP and LKP must overcome the barriers present in the small intestine to achieve systemic
58 delivery in order to illicit hypotensive action. Oral delivery requires a peptide to be stable in
59 stomach acid, soluble at small intestinal fluid pH, to be resistant to peptidase enzymes in the
60 small intestinal lumen and brush border, and to have sufficient muco-diffusion and epithelial
61 permeability [10]. Peptides typically have low and variable intestinal epithelial permeability,
62 which results in poor oral bioavailability due to their large molecular weight (MW),
63 hydrophilicity, and susceptibility to enzymatic degradation [11]. However, both IPP and LKP
64 have relatively low MWs (325 Da and 356 Da respectively), and therefore may not encounter
65 the same permeability issues as larger peptides. In addition, the presence of the cyclic amino
66 acid, proline, in the primary structure of IPP and LKP provides resistance to enzymatic
67 degradation in the small intestine [12-14]. The possible permeability routes for IPP and LKP

68 include likely contributions from the H⁺ coupled di- and tripeptide co-transporter PepT1
69 (encoded by SLC15A1) [15], and paracellular transport [16, 17].

70

71 There is evidence of both paracellular- and PepT1-mediated uptake of other di- and
72 tripeptides, although there is debate on which route is of more significance [16, 18, 19].

73 Contribution of PepT1-mediated uptake can be determined *in vitro* in Caco-2 monolayers by
74 saturating PepT1 with glycyl-sarcosine (Gly-Sar), a high affinity dipeptidyl competitive

75 inhibitor and substrate [20, 21]. A decrease in permeability in the presence of Gly-Sar
76 suggests that the candidate peptide is a substrate for PepT1 [22, 23]. However, this

77 conclusion for many molecules relies mainly on tests using Caco-2 monolayers, which may
78 not correlate with *in vivo* in terms of PepT1 expression and function. Foltz *et al.*

79 demonstrated that there was low permeability of IPP across Caco-2 monolayers (apparent
80 permeability coefficient, P_{app} = 1 x 10⁻⁸ cm/s) and across distal rat jejunum mounted in Ussing

81 chambers (P_{app} = 5 x 10⁻⁸ cm/s), but they did not test its permeability in the presence of a
82 PepT1 inhibitor [19]. PepT1 functions in conjunction with the Na⁺/H⁺ exchanger (NHE3),

83 which contributes to the small intestinal epithelial acidic microclimate in the immediate layer
84 above the epithelium, thereby providing protons for inwardly-directed symport with

85 substrates [24]. Despite the presence of an unstirred layer, the microclimate is not present in
86 filter-grown Caco-2 monolayers, perhaps due to the lack of goblet cells to produce overlying

87 mucus [25, 26].

88

89 The aim of this study was to determine the extent and major route(s) of permeability of [³H]-
90 IPP and [³H]-LKP in Caco-2 monolayers, isolated rat jejunal tissue in Ussing chambers, and

91 intra-jejunal instillations in rats. In order to assess the degree of permeation due to PepT1-

92 mediated uptake, Gly-Sar was tested as an inhibitor of inward peptide flux in each model. An
93 apical-side pH of 6.5 is required to mimic the small intestinal acidic microclimate [27],
94 therefore, the effect of apical-side/luminal buffer pH of either 6.5 or 7.4 was tested in each
95 model. The effect of these buffers on the jejunal acidic microclimate was also directly
96 assessed in rat jejunal sacs as it was not possible to measure surface pH in Ussing chambers.
97 Some transport models have limitations therefore it is necessary to assess the transport of IPP
98 and LKP in more than one experimental model. The data show that PepT1 plays an important
99 role in the intestinal uptake of these molecules, and that, based on the *in vitro* P_{app} values and
100 levels of radiolabelled peptide achieved in plasma following intestinal instillations, both IPP
101 and LKP have good permeability.

102 **2 Materials**

103 **2.1 Reagents and Chemicals**

104 [³H]-IPP and [³H]-LKP (specific activity 21 Ci/mmol) were obtained from Cambridge
105 Research Biochemicals (Billingham, UK). [¹⁴C]-mannitol (specific activity 250 μ Ci/mmol)
106 was obtained from Perkin Elmer (UK). All other reagents, chemicals, and solvents were
107 analytical grade from Sigma-Aldrich (UK). Caco-2 cells (passage 48-58) were obtained from
108 European Collection of Cell Cultures (Salisbury, UK).

109 **2.2 Caco-2 cell monolayers**

110 Caco-2 cells were grown in Dulbecco's Modified Eagle Medium (DMEM) with L-glutamine
111 (2 mM), 1% non-essential amino acids, penicillin (100 U)/streptomycin (100 μ g/ml) and 10%
112 foetal bovine serum (Gibco, Biosciences Ireland) on 75 cm² tissue culture flasks at 95%
113 O₂/5% CO₂ at 37°C in a humidified environment. Cells were seeded at a density of 3 x 10⁵
114 cells/well on 1.12 cm² Transwell[®] filters (polycarbonate, pore size 0.4 μ m) (Corning Costar
115 Corp., USA) and grown for 21 days in DMEM for transport experiments [28]. Transepithelial

116 electrical resistance (TEER, $\Omega \cdot \text{cm}^2$) was measured across the monolayers using an EVOM[®]
117 voltohmmeter with a chopstick electrode (EVOM[®], WPI, UK). TEER measurements were
118 made prior to transport studies and then every 30 min over a period of 120 min to confirm
119 monolayer integrity.

120 **2.3 *Caco-2 monolayer transport studies***

121 Apical-to-basolateral (A to B) transport of [³H]-IPP, [³H]-LKP and [¹⁴C]-mannitol were
122 examined across monolayers. The transport buffer consisted of HBSS supplemented with
123 12.5 mM glucose and either 25 mM HEPES (pH 7.4) or 10 mM 2-(N-
124 morpholino)ethanesulfonic acid (MES, pH 6.5) [26, 28]. DMEM was replaced with HBSS
125 and equilibrated for 30 min in the presence or absence of apical-side 10 mM Gly-Sar in
126 HBSS. This was carried out in the presence of apical-side pH adjustment (apical side
127 contained HBSS at pH 6.5, basolateral side contained HBSS at pH 7.4) or under standard pH
128 conditions (both apical and basolateral sides contained HBSS at pH 7.4). At time zero, [³H]-
129 IPP (1 $\mu\text{Ci}/\text{ml}$; 3 μM), [³H]-LKP (1 $\mu\text{Ci}/\text{ml}$; 3 μM) or [¹⁴C]-mannitol (0.1 $\mu\text{Ci}/\text{ml}$) was added
130 to the apical side. Basolateral samples were taken every 30 min for 120 min and apical
131 samples were taken at 0 and 120 min in order to calculate the P_{app} . Withdrawn samples were
132 replaced with an equal volume of fresh HBSS. Both basolateral and apical samples of 100 μl
133 were mixed with 5 ml scintillation fluid and measured in a liquid scintillation counter
134 (Packard Tricarb 2900 TR). Basal transepithelial electrical resistance (TEER) values were
135 required to be $> 1400 \Omega \cdot \text{cm}^2$ in order to be included [29]. The P_{app} for each marker was
136 calculated according to the following equation:

$$137 \quad P_{\text{app}} = \frac{dQ}{dt} \frac{1}{A \cdot C_0} \quad (1)$$

138 where dQ/dt is the transport rate across the epithelium, A is the surface area (1.12 cm^2) and
139 C_0 is the starting concentration of flux marker on the apical side [28]. Caco-2 transport
140 experiments were run in triplicate ($n=3$) with 3 independent replicates.

141 **2.4 Rat intestinal tissue mucosae: dissection and electrophysiology**

142 Studies were carried out in accordance with UCD Animal Research Ethics Committee
143 protocol (AREC 14-28-Brayden) and in adherence with the “Principles of Laboratory Animal
144 Care” (NIH Publication #85-23, revised in 1985). Male Wistar rats (250-350 g; Charles
145 River, UK and UCD Biomedical Facility, Ireland) were euthanised by stunning and cervical
146 dislocation in accordance with recommended procedures. Jejunum was removed 10-12 cm
147 proximal to the stomach, opened along the mesenteric border and rinsed with warm
148 oxygenated Krebs-Henseleit buffer (KH) [14]. Mucosae with underlying intact muscle was
149 mounted in Ussing chambers with a circular window area of 0.63 cm^2 [30], bathed bilaterally
150 with 5 ml KH and continuously gassed with 95% $\text{CO}_2/5\% \text{ O}_2$ and maintained at 37°C . The
151 transepithelial potential difference (PD; mV) and short circuit current (I_{sc} , μA) were
152 measured across jejunal tissue using a DVC-4000 voltage clamp apparatus (WPI, UK). After
153 an initial 30 min equilibration, PD and I_{sc} were used to calculate the TEER over 120 min
154 [31].

155 **2.5 Isolated rat jejunal mucosae transport studies**

156 Transepithelial permeability of [^3H]-IPP, [^3H]-LKP and [^{14}C]-mannitol were measured across
157 jejunal mucosae mounted in Ussing chambers. The apical-side transport buffers consisted of
158 KH (pH 7.4) or KH modified with 10 mM MES (pH 6.5), while the the basolateral buffer was
159 KH (pH 7.4) throughout [32]. Tissues were equilibrated for 30 min in the presence or absence
160 of 10 mM Gly-Sar on the apical side. At time zero, [^3H]-IPP (1 $\mu\text{Ci/ml}$; 3 μM), [^3H]-LKP (1
161 $\mu\text{Ci/ml}$; 3 μM) or [^{14}C]-mannitol (0.1 $\mu\text{Ci /ml}$) was added apically. Basolateral samples (100

162 μl) were taken every 30 min for 120 min and apical samples (100 μl) were taken at 0 and 120
163 min in order to calculate the P_{app} . Samples of 100 μl were mixed with 5 ml scintillation fluid
164 and read in a liquid scintillation counter as described above. The P_{app} for [^3H]-IPP, [^3H]-LKP
165 and [^{14}C]-mannitol was calculated according to equation (1) used for monolayers, the only
166 difference being that the surface area for jejunal mucosae was 0.63 cm^2 . Basal jejunal TEER
167 values were required to be $> 30 \Omega \text{ cm}^2$ or were otherwise excluded [30]. Jejunal mucosae
168 transport experiments were carried out as five independent replicates.

169 **2.6 Measurement of rat jejunal surface pH**

170 The pH of the jejunal surface was measured using a micro pH combination electrode (3.6 mm
171 diameter, Sigma Aldrich, UK) and a Hanna HI 2210 pH Meter [27]. Tissue was harvested,
172 flushed with pre-warmed PBS and a pH probe was inserted into the jejunal lumen to record
173 untreated native pH value. Non-everted gut sacs (5 cm in length) were prepared according to
174 previous methods [33], and injected with 0.25 ml of KH (pH 7.4) or KH (pH 6.5) with a 30G
175 needle and maintained in oxygenated KH for 120 min. The sacs and ligation was removed,
176 and flushed with pre-warmed PBS. The pH probe was inserted into the lumen and the pH
177 recorded. Measurements were recorded at 0 and 120 min after incubation. Experiments were
178 carried out using independent replicates from five animals.

179 **2.7 Rat intra-intestinal *in situ* jejunal instillations**

180 All animal experimental procedures in the study adhered to the EC Directive 86/609/EEC for
181 animal experiments and were performed in compliance with the Irish Health Products
182 Regulatory Authority animal licence number AE18982/P037. Male Wistar rats (Charles
183 River, UK) weighing 280-350 g were used. Animals were housed under controlled
184 environmental conditions regarding humidity and temperature with a 12:12 h light/dark cycle.
185 Rats received filtered water and standard laboratory chow *ad lib* and were fasted for 16-20 h

186 prior to procedure with free access to water. Anaesthesia was induced with isoflurane gas
187 (Iso-Vet, 1000 mg/g isoflurane liquid for inhalation, Piramal Healthcare, UK) at a rate of
188 4000 ml/min mixed with 4000 ml/min O₂ in an induction chamber. Anaesthesia was
189 maintained with isoflurane 2500 ml/min mixed with 1500 ml/min O₂ using vaporising unit
190 with a delivery mask (Blease Medical Equipment Ltd., UK). Animals were euthanised at the
191 end of the experiment by intracardiac injection of 0.4 ml pentobarbital sodium
192 (EUTHATAL™, Merial Animal Health Ltd., UK).

193 Isoflurane-anaesthetised rats were placed on a temperature controlled heat pad, and intra-
194 jejunal instillations were performed as previously described, but with minor modifications
195 [34]. Following a midline laparotomy, the jejunum was identified and tied off at both ends 5-
196 7cm apart with a size 4 braided silk suture. Test solutions of 300 µl of [³H]-IPP (8 µCi/kg; 24
197 µM) or [³H]-LKP (8 µCi/kg; 24 µM) in Dulbecco's Phosphate Buffered Saline (DPBS, pH
198 7.4) or DPBS buffered with 10 mM MES (pH 6.5), were injected into the lumen using a 1 ml
199 syringe fitted with a 30G needle. 100 mM Gly-Sar was solubilised in either DPBS adjusted to
200 pH 6.5 or in DPBS at pH 7.4 [35]. Blood samples (~400 µl) were taken via the retro-orbital
201 route at 0, 30, 60, 90 and 120 min into 1 ml Eppendorf tubes and stored on ice at 2-8°C prior
202 to centrifugation (6500g, 5 min) and serum collection. Serum (100 µl) was mixed with 5 ml
203 scintillation fluid and read in a liquid scintillation counter. Levels of [³H]-IPP and [³H]-LKP
204 in serum samples were used to determine the area under the curve (AUC).

205 **2.8 *Histology and immunofluorescence of monolayers and jejunal tissue***

206 Following the studies in jejunal tissue in Ussing chambers and intra-jejunal instillations,
207 tissue was immersed in 10% (v/v) buffered formalin for 48 h. Tissues were prepared,
208 paraffin-embedded, cut with a microtome, and dried overnight at 60°C. Tissues were stained
209 with haematoxylin and eosin (H&E), Alcian blue and neutral red. Slides were visualised

210 under a light microscope (NanoZoomer 2.0-HT light microscopy, Hamamatsu) and images
211 were taken with high-resolution camera (Micropublisher 3.3 RTV, QImaging) and Image-
212 Pro® Plus version 7.1 (Media Cybernetics Inc., USA) acquisition software.

213 The localisation of PepT1 and occludin was determined by immunofluorescence microscopy
214 as previously described [36, 37], but with modifications. Briefly, paraffin- embedded jejunal
215 segments on charged slides were deparaffinised with xylene and ethanol before incubation in
216 pre-warmed (90°C) 10 mM sodium citrate and 2 mM citric acid buffer for 10 min, and then
217 cooled to room temperature over 30 min. Caco-2 cell monolayers were fixed in ice cold
218 methanol for 30 min and washed with PBS. The non-specific background was blocked by
219 incubation with 5% bovine serum albumin in PBS for 45 min at room temperature. The
220 sections were incubated with rabbit polyclonal antibody (Santa Cruz Biotech, Germany)
221 against PepT1 at 4°C overnight. PepT1 was probed with Alexa Fluor® 488-conjugated
222 secondary goat anti-rabbit IgG antibody (Thermo Fisher Scientific, USA). Caco-2 cells were
223 probed with Alexa Fluor® 494 mouse monoclonal antibody (Thermo Fisher Scientific, USA)
224 against occludin. The slides were washed and mounted in Dako fluorescence mounting media
225 (Dako Diagnostics Ireland Ltd, Ireland). Slides incubated without primary antibody were
226 used as negative controls. Epi-fluorescent analysis was performed with Zeiss Axioplan 2
227 microscope (Zeiss, Germany)

228 **2.9 Statistical Analysis**

229 Statistical analysis was carried out using Prism-5[®] software (GraphPad, San Diego, USA)
230 using one-way ANOVA and Dunnett's *post hoc* test. Results are presented as the mean ±
231 standard error of the mean (SEM). A significant difference was considered present if $P <$
232 0.05.

233

234 **3 Results**

235 **3.1 Transport of [³H]-IPP, [³H]-LKP and [¹⁴C]-mannitol across Caco-2 monolayers**

236 The mean basal TEER value for Caco-2 monolayers was $1980 \pm 104 \Omega \text{ cm}^2$ (n=36), within
237 the range reported by this lab [29] and others [38]. The addition of Gly-Sar had no effect on
238 TEER and values remained similar to that of untreated monolayers (data not shown).
239 Modification of apical buffer pH from 7.4 to 6.5 also had no effect on TEER, with no
240 difference noted between groups incubated with apical side buffers of either pH value after
241 120 min. The P_{app} for [³H]-IPP, [³H]-LKP and [¹⁴C]-mannitol was measured in the A to B
242 direction using apical side buffers at pH values of either 7.4 or 6.5 (Table 1). When
243 monolayers were pre-incubated with Gly-Sar (10 mM) when the apical side buffer pH was
244 6.5, there was a decrease in the P_{app} of [³H]-IPP by 42% (Fig. 1A) and [³H]-LKP by 52% (Fig
245 1B). However, when the apical side buffer pH was 7.4, there was no reduction in the P_{app} of
246 either [³H]-IPP or [³H]-LKP in the presence of Gly-Sar. This indicates that enabling Gly-Sar
247 inhibition of PepT1-mediated uptake of [³H]-IPP and [³H]-LKP by monolayers requires
248 acidic buffer (pH 6.5) conditions on the apical side. To determine if the pH of 6.5 and pre-
249 incubation of Gly-Sar effected the integrity of the monolayer or paracellular transport, the
250 P_{app} of [¹⁴C]-mannitol was also tested under the same conditions (Fig 1C). Neither an apical
251 side buffer pH of 6.5 nor Gly-Sar pre-incubation altered the P_{app} of [¹⁴C]-mannitol,
252 suggesting there was no effect of either condition on paracellular transport.

253 When the apical side buffer pH was 7.4, [³H]-IPP had a higher P_{app} value ($14.8 \times 10^{-6} \text{ cm/s}$)
254 than when the apical side buffer pH was 6.5 ($6.8 \times 10^{-6} \text{ cm/s}$) (Table 1). This is likely due to
255 the physicochemical characteristics of the tripeptide in apical side buffers with pH 6.5 or 7.5
256 which can affect the permeation if there is a net neutral or ionised charge [39]. Overall, this

257 suggests [³H]-IPP and [³H]-LKP both use PepT1-mediated uptake, when the apical side pH is
258 6.5.

259 **3.2 Transport of [³H]-IPP, [³H]-LKP and [¹⁴C]-mannitol across isolated rat jejunal** 260 ***mucosae in Ussing chambers***

261 The basal TEER for isolated rat jejunal mucosae was $37 \pm 9 \Omega \text{ cm}^2$ (n=40), within the
262 acceptable range [30]. Jejunal TEER gradually decreased over 120 min to 70-80% of the
263 initial basal value in all conditions. The addition of Gly-Sar and/or modification of apical
264 buffer pH from 7.4 to 6.5 had no effect on TEER, and there was no difference in TEER
265 between groups after 120 min (data not shown). The P_{app} of [³H]-IPP, [³H]-LKP and [¹⁴C]-
266 mannitol was obtained in the A to B direction across isolated rat jejunal mucosae using apical
267 side pH buffers of either 7.4 or 6.5 (Table 2). When tissue was pre-incubated with Gly-Sar
268 (10 mM), a decrease was observed in the P_{app} of [³H]-IPP (Fig 2A) and [³H]-LKP (Fig 2B) at
269 apical buffer pH values of either 7.4 or 6.5. There was no change in the P_{app} of [¹⁴C]-mannitol
270 in the presence or absence of Gly-Sar or when the apical buffer pH value was either 7.4 or 6.5
271 (Fig 2C). To assess the effects of an apical side buffer on the jejunal acidic microclimate, rat
272 jejunal non-everted sacs were prepared, and the surface pH was measured before and after
273 apical addition of KH buffers of 6.5 and 7.4 (Fig 3). The initial jejunal surface pH after the
274 tissue was harvested was 6.14 ± 0.02 . After 120 min incubation with the apical buffers,
275 surface pH increased to 6.29 ± 0.05 (for buffer pH 6.5) and to 6.49 ± 0.04 (for buffer pH 7.4).
276 Therefore, maintenance of the acidic surface pH above the epithelium was still achieved even
277 if the buffer of pH 7.4 was present for 120 min. This accounts for the decrease in P_{app} of [³H]-
278 IPP and [³H]-LKP in the presence of Gly-Sar in jejunal mucosae when the apical side buffer
279 pH was 7.4 due to maintenance of the acidic microclimate.

280

281 3.3 *Absorption of [³H]-IPP and [³H]-LKP from rat intra-jejunal instillations*

282 Intra-jejunal instillations were performed to further investigate the effects of altering apical
283 side buffer pH on absorption of [³H]-IPP and [³H]-LKP when co-administered with Gly-Sar
284 (100 mM) in buffers with pH values of either 7.4 or 6.5 (Table 3). Plasma AUC of [³H]-IPP
285 and [³H]-LKP decreased when co-administered with Gly-Sar in both buffers at pH 6.5 and
286 7.4 (Fig 4A and B). When apical buffer pH solutions were changed from 7.4 to 6.5, there was
287 no difference between the AUC values of groups in the absence of Gly-Sar. This indicates
288 that the jejunal acid microclimate was intact even at a apical buffer pH of 7.4 [40].

289

290 3.4 *Histology and immunofluorescence analysis of jejunal tissue and monolayers*

291 Histology analysis was used to assess the effects apical side buffer pH of 6.5 or 7.4 on jejunal
292 mucosae following 120 min exposure in both Ussing chambers and jejunal instillations.
293 Morphology of intestinal villi was unaffected across all experimental conditions;
294 representative images are shown (Fig. 5). Mucus secretion was assessed with Alcian blue and
295 neutral red staining. No histological changes were noted in the presence or absence of Gly-
296 Sar and with apical buffer pH of 6.5 or 7.4. There was no effect on mucus secretion, villi
297 depth, or cell sloughing when exposed to the different experimental conditions. To confirm
298 PepT1 expression in all three models, immunofluorescence was performed on Caco-2
299 monolayers and on jejunal mucosae from Ussing chamber experiments and instillations
300 following 120 min exposure to apical side buffer of 7.4. PepT1 expression was lower in
301 Caco-2 monolayers (Fig. 6A) compared to jejunal tissue in Ussing chambers (Fig. 6B) and
302 instillations (Fig. 6C). PepT1 was abundantly present in epithelia along the villi in jejunal
303 tissue, whereas a lower intensity was present across monolayers. Even though Caco-2 cells

304 are of colonic origin, they have been shown to express small intestinal transporters including
305 PepT1 at variable levels [41].

306 4 Discussion

307 It has been reported that the intestinal transport routes exploited by tripeptides include both
308 paracellular and PepT1-mediated transport [16, 18, 42]. Paracellular permeability was
309 assessed *in vitro* in Caco-2 monolayers by measuring mannitol permeability and TEER [28],
310 whereas PepT1-mediated uptake was assessed by Gly-Sar inhibition of substrate transport
311 [28]. Gly-Sar is a high affinity substrate for PepT1 [28], and competitively inhibits uptake of
312 other PepT1 substrates including IPP and LKP. Reductionist models such as Caco-2
313 monolayers lack complexities of more physiologically relevant models such as isolated
314 intestinal tissue in Ussing chambers and *in vivo* in situ intra-intestinal delivery. Caco-2
315 monolayers lack villi formation (although microvilli are present), PepT1 expression varies
316 (moderate to high), and epithelial cell types are limited to enterocytes [41]. *In vivo* the
317 intestinal epithelia is comprised of enterocytes, goblet cells, and Paneth cells [25, 43].
318 Although the Caco-2 monolayer has an unstirred water layer, it lacks the unstirred acidic
319 microclimate which is required for H⁺ coupled transporters: PepT1, the amino acid co-
320 transporter (PAT1), and NHE3 [44]. Therefore, to elucidate the route of transport of IPP and
321 LKP, permeability needs to be assessed across a combination of Caco-2 monolayers as well
322 as isolated jejunal mucosae and *in situ* intra-jejunal instillations. Brandsch has further
323 suggested that prior to assigning a molecule as a PepT1 substrate, there is a need for detailed
324 transport studies in mammalian cells (Caco-2 expressing PepT1) or *Xenopus laevis* oocytes
325 transfected with PepT1 [45].

326

327 Other studies have investigated PepT1-mediated uptake of molecules across isolated
328 intestinal tissue in Ussing chambers. Examples include: Gly-Sar flux across isolated pig
329 jejunum [46] and across isolated jejunum from PepT1^{+/+} and PepT1^{-/-} mice [47], as well as

330 ceftibuten flux across isolated rat jejunum [48]. Here we show PepT1 contributes, at least in
331 part to the uptake of IPP and LKP across isolated rat jejunal mucosae, and this inhibition of
332 PepT1 by Gly-Sar was detected in apical side buffers of both pH 7.4 or 6.5. This proved not
333 to be the case in Caco-2 monolayers, most likely due to the absence of mucus and the
334 unstirred layer which assists the maintenance of an acidic microclimate in the small intestine.
335 The mechanism by which the acidic microclimate is generated is thought to depend on
336 transmembrane H⁺ secretion by NHE3 into the negatively charged mucus layer [49]. The
337 presence of jejunal mucus, if undisturbed during the mounting process in Ussing chambers,
338 may have retained the unstirred layer, and its acidic microclimate pH at the apical surface
339 was likely maintained even when apical buffer pH was 7.4. Goblet cells are present in jejunal
340 mucosae which continue to secrete mucus in the Ussing chamber as observed by histological
341 analysis. Increased pH in the jejunal microclimate has previously been reported and is
342 dependent on the buffer [50]. Increasing small intestinal luminal pH increases surface pH
343 somewhat, but the acidic microclimate is maintained as previously demonstrated [51].
344 Addition of the mucolytic, *N*-acetyl-L-cysteine (5%), increased the pH of the microclimate in
345 rats, further suggesting the role the mucus layer plays in maintaining the microclimate [52].

346

347 The addition of cephalixin, an established substrate of PepT1, also inhibited the transport of
348 [³H]-Gly-Sar when apical buffer pH was 7.4 across isolated mouse proximal jejunum in
349 Ussing chambers [53]. This is likely due to the continued presence of the acidic jejunal
350 microclimate even in buffers of pH 7.4, and is in line with our findings. Previous studies
351 demonstrated a minor increase in the rat jejunal microclimate pH due to increasing apical pH
352 and indeed, the loss of acidity in the microclimate only occurred at an apical pH of 9 [52].
353 Addition of the bile salt, sodium deoxycholate did not influence the pH of the microclimate in
354 the rat jejunum [54]. However, Lucas *et al.* determined that in gastrointestinal diseases such

355 as Crohn's and coeliac disease, the microclimate is less acidic (pH 6.5 and 6.2 respectively)
356 compared to that of healthy human volunteers (pH 5.9) [55]. This can indirectly impede
357 uptake of tripeptides due to loss of pH gradient across the intestinal epithelium.

358

359 In situ and *in vivo* models are essential for the characterisation of PepT1-mediated uptake of
360 substrates. When 100 mM Gly-Sar was co-administered with IPP or LKP in instillations, a
361 decrease in [³H]-IPP and [³H]-LKP rat blood plasma was observed. The permeability of the
362 prodrug Val-Val-sanquinivir was decreased in the presence of Gly-Sar in a rat intestinal
363 perfusion study by 68% [56]. Furthermore, blood plasma concentration of cefditoren
364 significantly decreased when co-administered with Gly-Sar in rat intestinal loops [57]. Glyco-
365 trans-4-L-hydroxyprolyl-L-serine (JBP485) blood plasma concentration was decreased when
366 co-administered with Gly-Sar in a rat intestinal perfusion study [58]. Although the in situ rat
367 loop-gut instillations can display large variations in permeability [19], numerous studies show
368 consistency between various *in vivo* jejunal models of PepT1-mediated absorption and
369 inhibition by Gly-Sar [56-58]. Rational design of inhibitors of PepT1 such as, Lys[Z(NO₂)]-
370 Pro, have been tested but failed to fully inhibit inward dipeptide uptake in line with Gly-Sar
371 inhibition [59]. For example, valacyclovir absorption was reduced (50%) by co-
372 administration of Gly-Sar in normal mice [60]. In the same study, valacyclovir absorption
373 was reduced to just 10% in a PepT1 knockout mice using jejunal perfusion. In this study,
374 [³H]-IPP and [³H]-LKP were reduced by 30-40% in the presence of Gly-Sar, this data may
375 suggest that they can also permeate paracellularly due to their low MW and hydrophilicity.

376

377 It is possible that intake of substrates which compete for PepT1 (such as dietary protein
378 sources), may lead to a reduced oral bioavailability of drugs and bioactives which target

379 uptake via PepT1. Matsui *et al.* reported a loss of hypotensive action from captopril when co-
380 administered with the antihypertensive dipeptide, Val-Tyr (VY), in the spontaneously
381 hypertensive rat (SHR), in contrast with effects seen with either agent alone [61]. The authors
382 suggested this was due to competition between captopril and VY for PepT1, and cautioned
383 that subjects treated with ACE inhibitors for hypertension should avoid combined intake of
384 foods rich in small peptides. On the other hand, when IPP was orally administered in a
385 protein or high fibre meal to pigs, a 1.6-fold and 1.2-fold increase in bioavailability was
386 observed [62]. It is possible that the composition of the meal will have resulted in delayed
387 gastric emptying leading to prolonged exposure time for IPP at the intestinal epithelia.

388

389 Overall, it was shown that [³H]-IPP and [³H]-LKP were highly permeable even when
390 inhibited with Gly-Sar in each model. Previously, Foltz *et al.* reported P_{app} values for IPP as 1
391 $\times 10^{-8}$ cm.s⁻¹ (Caco-2 monolayers) and 5 $\times 10^{-8}$ cm.s⁻¹ (isolated rat jejunal tissue in Ussing
392 chambers) [19]. The large difference between IPP P_{app} values in Caco-2 monolayers may be
393 due to low PepT1 expression in the Foltz study [41]. However, the studies used different
394 methods to quantify permeability, here the [³H] label was directly measured, while in the
395 Foltz study IPP was column purified and quantified by LC-MS [19]. Conversely, the values
396 reported here are in line with reported values for bioactive peptides across Caco-2
397 monolayers (P_{app} values ranging from 0.9 – 12.4 $\times 10^{-6}$ cm.s⁻¹) [63-66], and known PepT1
398 substrates across isolated jejunal tissue in Ussing chambers (P_{app} values ranging from 0.5 –
399 4.6 $\times 10^{-6}$ cm.s⁻¹) [61, 67, 68].

400

401 **5 Conclusions**

402 The routes of intestinal permeation of food-derived bioactive peptides, IPP and LKP were
403 investigated. Comparative test models *in vitro*, *ex vivo* and *in vivo* transport across intestinal
404 epithelia were utilised. Gly-Sar reduced the permeability of IPP and LKP in Caco-2
405 monolayers when the apical buffer pH was 6.5 but not when the apical buffer pH was 7.4. In
406 isolated rat jejunum in Ussing chambers and *in situ* intra-jejunal instillations, Gly-Sar
407 reduced IPP and LKP permeability in a nominally pH-independent manner (pH 6.5 or 7.4).
408 On closer analysis, this was likely due to the presence of an intact acidic jejunal microclimate
409 even when apical buffer pH was 7.4 in the jejunal tissue models. [¹⁴C]-mannitol permeability
410 and TEER was unaffected by the presence or absence of Gly-Sar and/or when apical buffer
411 pH was 6.5 or 7.4 in the *in vitro* studies. Overall, IPP and LKP permeate both by PepT1-
412 mediated uptake and via the paracellular route in the small intestine and are highly
413 permeable. A combination of the three transport models used in this study may be useful for
414 investigating the transport of other bioactive di- and tripeptides.

415

416 **Acknowledgements**

417 This study was supported by the Irish Department of Agriculture Food Institutional Research
418 Measure (FIRM) grant ‘NUTRADEL,’ grant number 11F042. We thank Mrs Margot Coady
419 for assistance with the histology. The authors have declared no conflict of interest.

420

421 **Figure Captions**

422 **Fig 1.** Effect of apical side buffer pH and/or Gly-Sar (10 mM) pre-incubation on the P_{app}
423 values of **A** [^3H]-IPP, **B** [^3H]-LKP and **C** [^{14}C]-mannitol across Caco-2 monolayers obtained
424 over 120 min. One-way ANOVA with Dunnett's multiple comparison; *** $P < 0.001$, ns =
425 not significant compared with control. Each value represents the mean \pm SEM, $n = 3$, with 3
426 independent replicates.

427 **Fig 2.** Effect of apical side buffer pH and/or Gly-Sar (10 mM) pre-incubation on the P_{app}
428 values of **A** [^3H]-IPP, **B** [^3H]-LKP and **C** [^{14}C]-mannitol across isolated rat jejunal tissue
429 obtained over 120 min. One-way ANOVA with Dunnett's multiple comparison; ** $P < 0.01$,
430 *** $P < 0.001$, ns = not significant compared with control. Each value represents the mean \pm
431 SEM, $n = 5$ independent replicates.

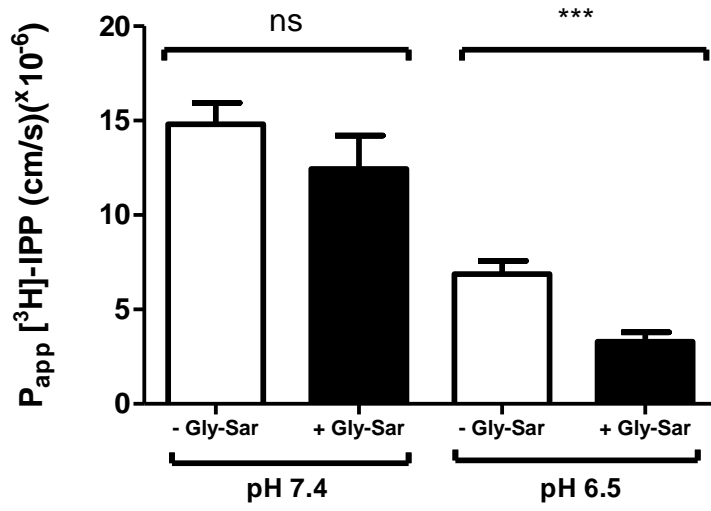
432 **Fig 3.** Effect of apical side buffer pH on the surface microclimate pH of isolated rat jejunal
433 sacs. The pH was measured at 0, and 120 min in pH of 6.5 or 7.4. One-way ANOVA with
434 Dunnett's multiple comparison; * $P < 0.05$, *** $P < 0.001$, compared with control (0 min).
435 Each value represents the mean \pm SEM, $n = 6$ independent experiments.

436 **Fig 4.** Effect of apical side buffer pH and/or the presence of Gly-Sar (100 mM) on the AUC
437 of plasma levels of **A** [^3H]-IPP and **B** [^3H]-LKP obtained over 120 min following jejunal
438 instillations to rats. One-way ANOVA with Dunnett's multiple comparison; ** $P < 0.01$, ***
439 $P < 0.001$, compared with control. Each value represents the mean \pm SEM, $n = 6$ independent
440 experiments.

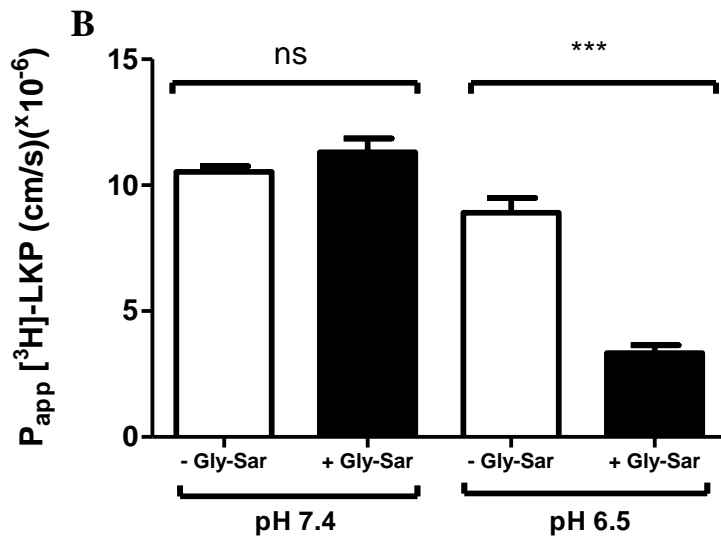
441 **Fig 5.** Alcian blue and neutral red-stained representative light micrographs of rat jejunal
442 tissue after 120 min in Ussing chambers (*ex vivo*) and instillations (*in vivo*) when apical side
443 buffer pH was 7.4 and 6.5, size bar indicates 100 μm .

444 **Fig 6.** Representative immunofluorescence analysis of PepT1 expression: (A) Caco-2
445 monolayers, (B) jejunal mucosae from Ussing chambers, and (C) jejunal instillations after
446 120 min exposure to pH of 7.4. PepT1 proteins are stained green and tight junctions are
447 stained red in monolayers. For interpretation of the colour, the reader is referred to the web
448 version of this article.

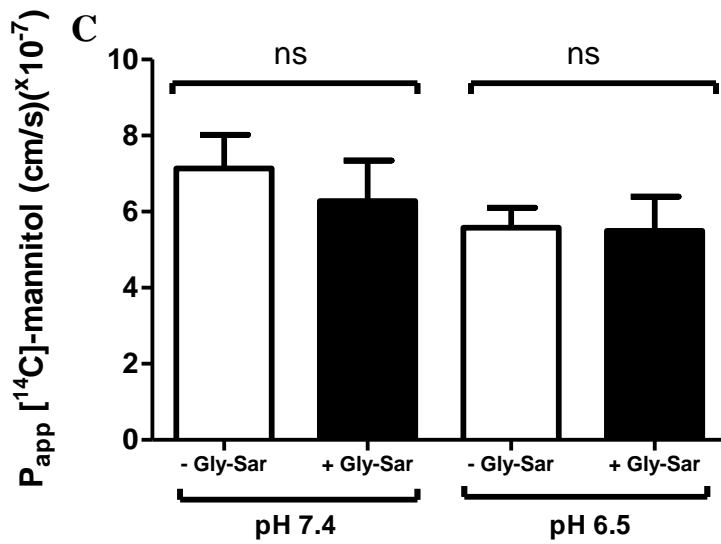
Fig 1 A



449

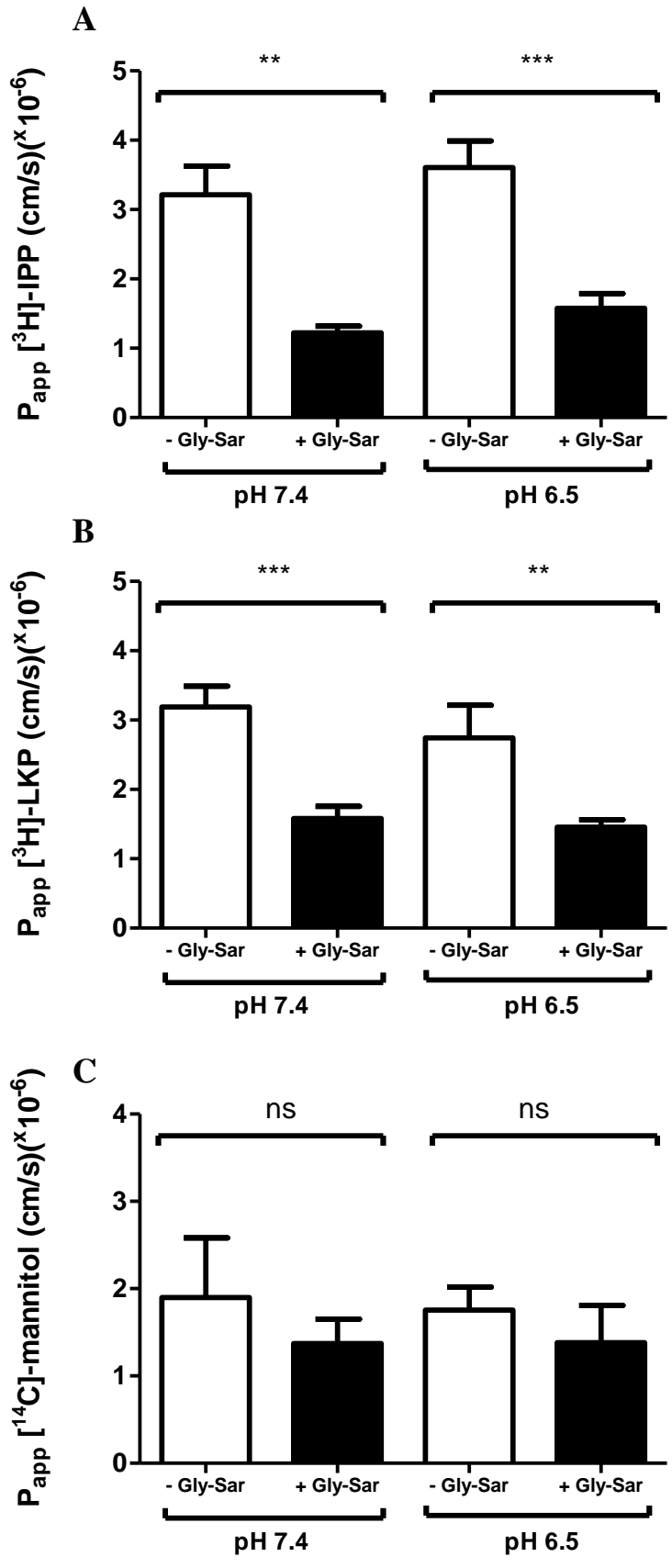


450



451

Fig 2

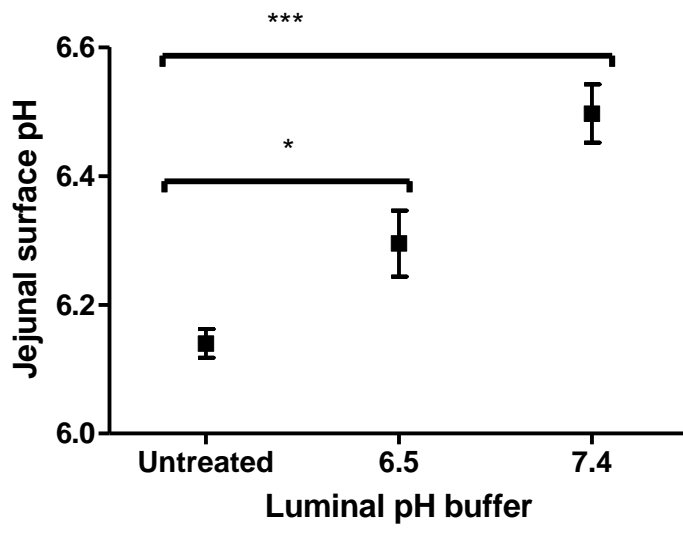


452

453

454

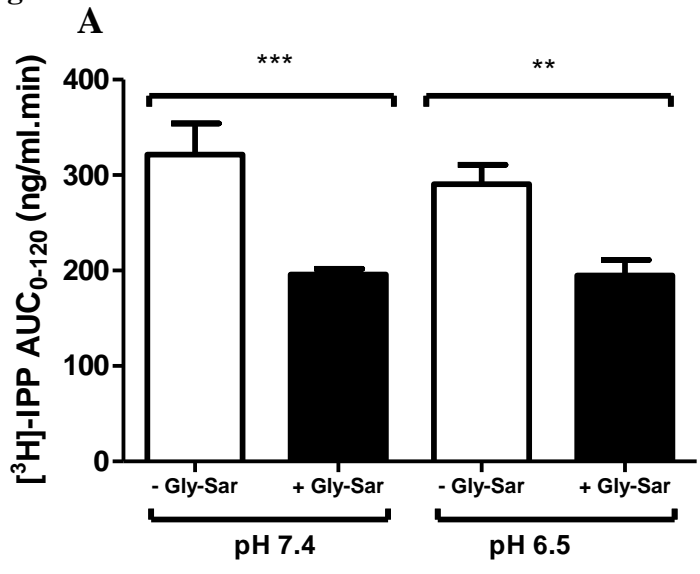
455 **Fig 3**



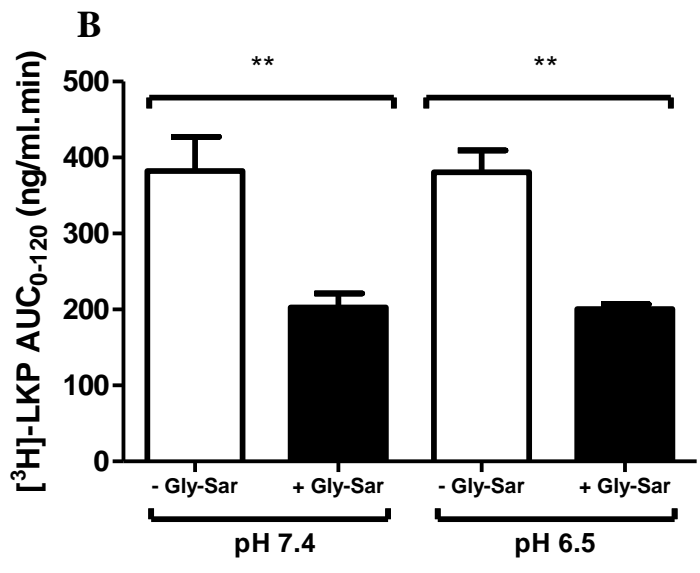
456

457

458 Fig 4



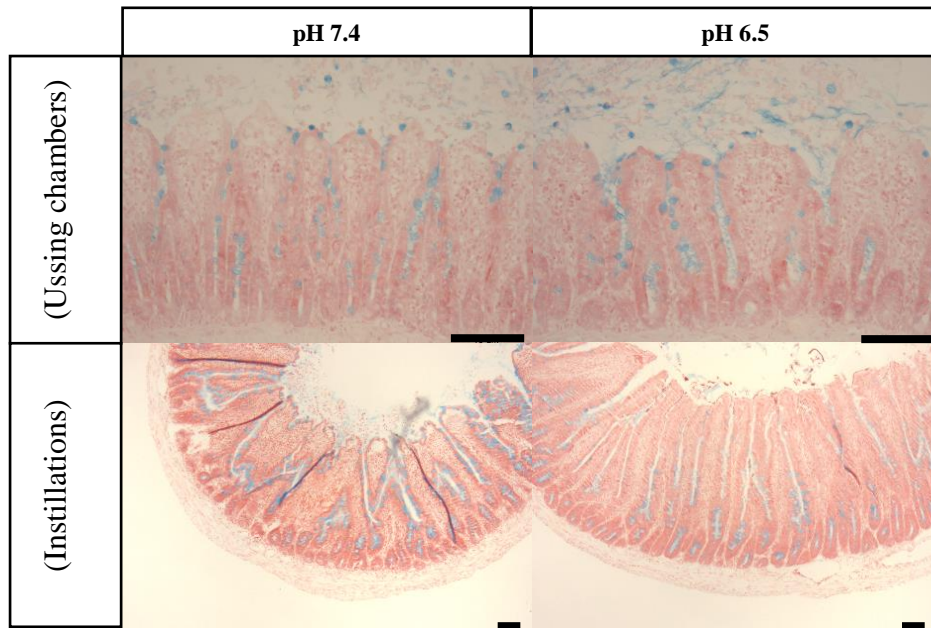
459



460

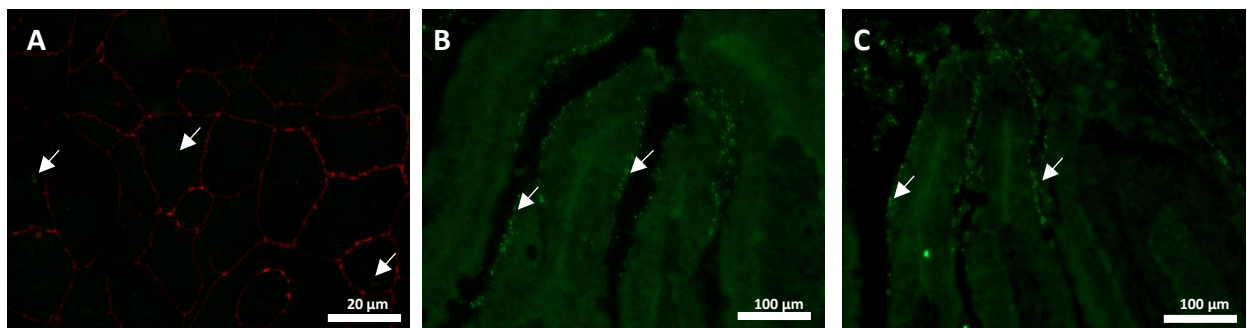
461

462 **Fig 5**



463

464 **Fig 6**



465

466

467 **Table 1** – Effect of apical side buffer pH and/or Gly-Sar (10 mM) on the P_{app} values of [^3H]-
 468 IPP, [^3H]-LKP and [^{14}C]-mannitol across Caco-2 monolayers obtained over 120 min periods.

Gly-Sar	pH	[^3H]-IPP P_{app} ($\times 10^{-6}$ cm.s $^{-1}$)	[^3H]-LKP P_{app} ($\times 10^{-6}$ cm.s $^{-1}$)	[^{14}C]-mannitol P_{app} ($\times 10^{-7}$ cm.s $^{-1}$)
(-)	7.4	14.8 \pm 1.1	10.5 \pm 0.2	7.1 \pm 0.8
(+)	7.4	12.4 \pm 1.7	11.3 \pm 0.6	6.3 \pm 1.1
(-)	6.5	6.8 \pm 0.7	8.9 \pm 0.6	5.6 \pm 0.5
(+)	6.5	3.3 \pm 0.5 ***	3.4 \pm 0.3 ***	5.5 \pm 0.9

One-way ANOVA with Dunnett's multiple comparison; *** $P < 0.001$, compared with control. Each value represents the mean \pm SEM, $n = 3$, with 3 independent replicates.

469

470 **Table 2** – Effect of an acidic apical side pH and/or Gly-Sar (10 mM) pre-incubation on the
 471 P_{app} values of [^3H]-IPP, [^3H]-LKP and [^{14}C]-mannitol across isolated rat jejunal tissue in
 472 Ussing chambers obtained over 120 min.

Gly-Sar	pH	[^3H]-IPP P_{app} ($\times 10^{-6}$ cm.s $^{-1}$)	[^3H]-LKP P_{app} ($\times 10^{-6}$ cm.s $^{-1}$)	[^{14}C]-mannitol P_{app} ($\times 10^{-6}$ cm.s $^{-1}$)
(-)	7.4	3.2 \pm 0.4	3.2 \pm 0.3	1.8 \pm 0.7
(+)	7.4	1.2 \pm 0.1 **	1.6 \pm 0.2 ***	1.4 \pm 0.3
(-)	6.5	3.6 \pm 0.4	2.8 \pm 0.4	1.7 \pm 0.3
(+)	6.5	1.6 \pm 0.2 ***	1.4 \pm 0.1 **	1.4 \pm 0.5

One-way ANOVA with Dunnett's multiple comparison; ** $P < 0.01$, *** $P < 0.001$, compared with control. Each value represents the mean \pm SEM, $n = 5$ independent replicates.

473

474

475 **Table 3** – Effect of apical side buffer pH and/or the presence of Gly-Sar (100 mM) on the
 476 AUC of plasma levels of [³H]-IPP and [³H]-LKP obtained in rat jejunal instillations over 120
 477 min.

Gly-Sar	pH	[³ H]-IPP AUC (ng/ml.min)	[³ H]-LKP AUC (ng/ml.min)
(-)	7.4	321 ± 32	382 ± 45
(+)	7.4	195 ± 5 ***	202 ± 18 **
(-)	6.5	290 ± 20	380 ± 29
(+)	6.5	195 ± 16 **	200 ± 6 **

One-way ANOVA with Dunnett's multiple comparison; ** P < 0.01, *** P < 0.001, compared with control. Each value represents the mean ± SEM, n =6 independent replicates.

478

479 **References**

- 480 [1] Nongonierma, A. B., FitzGerald, R. J., Bioactive properties of milk proteins in humans: A review.
481 *Peptides* 2015, 73, 20-34.
- 482 [2] Cicero, A. F., Aubin, F., Azais-Braesco, V., Borghi, C., Do the lactotripeptides isoleucine-proline-
483 proline and valine-proline-proline reduce systolic blood pressure in European subjects? A meta-
484 analysis of randomized controlled trials. *American journal of hypertension* 2013, 26, 442-449.
- 485 [3] Turpeinen, A. M., Jarvenpaa, S., Kautiainen, H., Korpela, R., Vapaatalo, H., Antihypertensive
486 effects of bioactive tripeptides - a random effects meta-analysis. *Annals of Medicine* 2013, 45, 51-56.
- 487 [4] Akhavan, T., Luhovyy, B. L., Brown, P. H., Cho, C. E., Anderson, G. H., Effect of premeal
488 consumption of whey protein and its hydrolysate on food intake and postmeal glycemia and insulin
489 responses in young adults. *Am J Clin Nutr* 2010, 91, 966-975.
- 490 [5] Goudarzi, M., Madadlou, A., Influence of whey protein and its hydrolysate on prehypertension
491 and postprandial hyperglycaemia in adult men. *International Dairy Journal* 2013, 33, 62-66.
- 492 [6] Nakamura, Y., Yamamoto, N., Sakai, K., Okubo, A., *et al.*, Purification and characterization of
493 angiotensin I-converting enzyme inhibitors from sour milk. *Journal of Dairy Science* 1995, 78, 777-
494 783.
- 495 [7] Fujita, H., Yoshikawa, M., LKPNM: a prodrug-type ACE-inhibitory peptide derived from fish
496 protein. *Immunopharmacology* 1999, 44, 123-127.
- 497 [8] Fujita, H., Yokoyama, K., Yoshikawa, M., Classification and antihypertensive activity of
498 angiotensin I-converting enzyme inhibitory peptides derived from food proteins. *Journal of food*
499 *science* 2000, 65, 564-569.
- 500 [9] Nakamura, Y., Yamamoto, N., Sakai, K., Takano, T., Antihypertensive effect of sour milk and
501 peptides isolated from it that are inhibitors to angiotensin I-converting enzyme. *J Dairy Sci* 1995, 78,
502 1253-1257.
- 503 [10] Moroz, E., Matoori, S., Leroux, J. C., Oral delivery of macromolecular drugs: Where we are after
504 almost 100years of attempts. *Adv Drug Deliv Rev* 2016, *In Press*.
- 505 [11] Maher, S., Duffy, B., Ryan, A., Brayden, D. J., Formulation strategies to improve oral peptide
506 delivery. *Pharmaceutical Patent Analyst* 2014, 3, 313-336.
- 507 [12] Ohsawa, K., Satsu, H., Ohki, K., Enjoh, M., *et al.*, Producibility and digestibility of
508 antihypertensive beta-casein tripeptides, Val-Pro-Pro and Ile-Pro-Pro, in the gastrointestinal tract:
509 analyses using an in vitro model of mammalian gastrointestinal digestion. *J. Agric. Food Chem.* 2008,
510 56, 854-858.
- 511 [13] Yaron, A., Naider, F., Proline-dependent structural and biological properties of peptides and
512 proteins. *Crit Rev Biochem Mol Biol* 1993, 28, 31-81.
- 513 [14] Gleeson, J. P., Heade, J., Ryan, S. M., Brayden, D. J., Stability, toxicity and intestinal permeation
514 enhancement of two food-derived antihypertensive tripeptides, Ile-Pro-Pro and Leu-Lys-Pro.
515 *Peptides* 2015, 71, 1-7.
- 516 [15] Omkvist, D. H., Larsen, S. B., Nielsen, C. U., Steffansen, B., *et al.*, A quantitative structure-activity
517 relationship for translocation of tripeptides via the human proton-coupled peptide transporter,
518 hPEPT1 (SLC15A1). *The AAPS journal* 2010, 12, 385-396.
- 519 [16] Satake, M., Enjoh, M., Nakamura, Y., Takano, T., *et al.*, Transepithelial transport of the bioactive
520 tripeptide, Val-Pro-Pro, in human intestinal Caco-2 cell monolayers. *Biosci Biotechnol Biochem* 2002,
521 66, 378-384.
- 522 [17] Miner-Williams, W. M., Stevens, B. R., Moughan, P. J., Are intact peptides absorbed from the
523 healthy gut in the adult human? *Nutrition research reviews* 2014, 27, 308-329.
- 524 [18] Gan, L. S., Niederer, T., Eads, C., Thakker, D., Evidence for predominantly paracellular transport
525 of thyrotropin-releasing hormone across Caco-2 cell monolayers. *Biochem. Biophys. Res. Commun.*
526 1993, 197, 771-777.

527 [19] Foltz, M., Cerstiaens, A., van Meensel, A., Mols, R., *et al.*, The angiotensin converting enzyme
528 inhibitory tripeptides Ile-Pro-Pro and Val-Pro-Pro show increasing permeabilities with increasing
529 physiological relevance of absorption models. *Peptides* 2008, 29, 1312-1320.

530 [20] Thwaites, D. T., Brown, C. D., Hirst, B. H., Simmons, N. L., H(+)-coupled dipeptide
531 (glycylsarcosine) transport across apical and basal borders of human intestinal Caco-2 cell
532 monolayers display distinctive characteristics. *Biochimica et biophysica acta* 1993, 1151, 237-245.

533 [21] Hong, S.-M., Tanaka, M., Koyanagi, R., Shen, W., Matsui, T., Structural design of oligopeptides
534 for intestinal transport model. *Journal of agricultural and food chemistry* 2016, 64, 2072-2079.

535 [22] Kovacs-Nolan, J., Zhang, H., Ibuki, M., Nakamori, T., *et al.*, The PepT1-transportable soy
536 tripeptide VPY reduces intestinal inflammation. *Biochimica et Biophysica Acta (BBA) - General*
537 *Subjects* 2012, 1820, 1753-1763.

538 [23] Fernández-Musoles, R., Salom, J. B., Castelló-Ruiz, M., Contreras, M. d. M., *et al.*, Bioavailability
539 of antihypertensive lactoferricin B-derived peptides: Transepithelial transport and resistance to
540 intestinal and plasma peptidases. *International Dairy Journal* 2013, 32, 169-174.

541 [24] Thwaites, D. T., Ford, D., Glanville, M., Simmons, N. L., H(+)/solute-induced intracellular
542 acidification leads to selective activation of apical Na(+)/H(+) exchange in human intestinal epithelial
543 cells. *J. Clin. Invest.* 1999, 104, 629-635.

544 [25] Kim, H. J., Ingber, D. E., Gut-on-a-Chip microenvironment induces human intestinal cells to
545 undergo villus differentiation. *Integrative biology : quantitative biosciences from nano to macro*
546 2013, 5, 1130-1140.

547 [26] Neuhoff, S., Ungell, A. L., Zamora, I., Artursson, P., pH-Dependent passive and active transport
548 of acidic drugs across Caco-2 cell monolayers. *European journal of pharmaceutical sciences : official*
549 *journal of the European Federation for Pharmaceutical Sciences* 2005, 25, 211-220.

550 [27] Lucas, M., Determination of acid surface pH in vivo in rat proximal jejunum. *Gut* 1983, 24, 734-
551 739.

552 [28] Hubatsch, I., Ragnarsson, E. G., Artursson, P., Determination of drug permeability and prediction
553 of drug absorption in Caco-2 monolayers. *Nature protocols* 2007, 2, 2111-2119.

554 [29] Petersen, S. B., Nolan, G., Maher, S., Rahbek, U. L., *et al.*, Evaluation of alkylmaltosides as
555 intestinal permeation enhancers: comparison between rat intestinal mucosal sheets and Caco-2
556 monolayers. *European journal of pharmaceutical sciences : official journal of the European*
557 *Federation for Pharmaceutical Sciences* 2012, 47, 701-712.

558 [30] Sjogren, E., Eriksson, J., Vedin, C., Breitholtz, K., Hilgendorf, C., Excised segments of rat small
559 intestine in Ussing chamber studies: A comparison of native and stripped tissue viability and
560 permeability to drugs. *Int. J. Pharm.* 2016, 505, 361-368.

561 [31] Cuthbert, A. W., Margolius, H. S., Kinins stimulate net chloride secretion by the rat colon. *Br J*
562 *Pharmacol* 1982, 75, 587-598.

563 [32] Zheng, Y., Benet, L. Z., Okochi, H., Chen, X., pH dependent but not P-gp dependent bidirectional
564 transport study of S-propranolol: the importance of passive diffusion. *Pharmaceutical research* 2015,
565 32, 2516-2526.

566 [33] Mateer, S. W., Cardona, J., Marks, E., Goggin, B. J., *et al.*, Ex vivo intestinal sacs to assess
567 mucosal permeability in models of gastrointestinal disease. *Journal of visualized experiments : JoVE*
568 2016, e53250.

569 [34] Aguirre, T. A. S., Rosa, M., Guterres, S. S., Pohlmann, A. R., *et al.*, Investigation of coco-glucoside
570 as a novel intestinal permeation enhancer in rat models. *Eur J Pharm Biopharm* 2014, 88, 856-865.

571 [35] Poirier, A., Belli, S., Funk, C., Otteneder, M. B., *et al.*, Role of the intestinal peptide transporter
572 PEPT1 in Oseltamivir absorption: In vitro and in vivo studies. *Drug Metab. Disposition* 2012, 40,
573 1556-1565.

574 [36] Long, D. J., Buggs, C., Microwave oven-based technique for immunofluorescent staining of
575 paraffin-embedded tissues. *Journal of molecular histology* 2008, 39, 1-4.

576 [37] Behrens, I., Kamm, W., Dantzig, A. H., Kissel, T., Variation of peptide transporter (PepT1 and
577 HPT1) expression in Caco-2 cells as a function of cell origin. *J. Pharm. Sci.* 2004, 93, 1743-1754.

578 [38] Marušić, M., Zupančič, T., Hribar, G., Komel, R., *et al.*, The Caco-2 cell culture model enables
579 sensitive detection of enhanced protein permeability in the presence of N-decyl- β -D-
580 maltopyranoside. *New Biotechnology* 2013, 30, 507-515.

581 [39] Duan, J., Xie, Y., Luo, H., Li, G., *et al.*, Transport characteristics of isorhamnetin across intestinal
582 Caco-2 cell monolayers and the effects of transporters on it. *Food Chem. Toxicol.* 2014, 66, 313-320.

583 [40] Lucas, M. L., Lei, F. H., Blair, J. A., The influence of buffer pH, glucose and sodium ion
584 concentration on the acid microclimate in rat proximal jejunum in vitro. *Pflügers Archiv* 1980, 385,
585 137-142.

586 [41] Hayeshi, R., Hilgendorf, C., Artursson, P., Augustijns, P., *et al.*, Comparison of drug transporter
587 gene expression and functionality in Caco-2 cells from 10 different laboratories. *European journal of*
588 *pharmaceutical sciences : official journal of the European Federation for Pharmaceutical Sciences*
589 2008, 35, 383-396.

590 [42] Foltz, M., van Buren, L., Klaffke, W., Duchateau, G. S., Modeling of the relationship between
591 dipeptide structure and dipeptide stability, permeability, and ACE inhibitory activity. *Journal of food*
592 *science* 2009, 74, H243-251.

593 [43] Kim, H. J., Li, H., Collins, J. J., Ingber, D. E., Contributions of microbiome and mechanical
594 deformation to intestinal bacterial overgrowth and inflammation in a human gut-on-a-chip.
595 *Proceedings of the National Academy of Sciences* 2016, 113, E7-E15.

596 [44] Anderson, C. M., Thwaites, D. T., Hijacking solute carriers for proton-coupled drug transport.
597 *Physiology (Bethesda, Md.)* 2010, 25, 364-377.

598 [45] Brandsch, M., Drug transport via the intestinal peptide transporter PepT1. *Current opinion in*
599 *pharmacology* 2013, 13, 881-887.

600 [46] Winckler, C., Breves, G., Boll, M., Daniel, H., Characteristics of dipeptide transport in pig jejunum
601 in vitro. *Journal of Comparative Physiology B* 1999, 169, 495-500.

602 [47] Nässl, A.-M., Rubio-Aliaga, I., Fenselau, H., Marth, M. K., *et al.*, Amino acid absorption and
603 homeostasis in mice lacking the intestinal peptide transporter PEPT1. *American Journal of Physiology*
604 *- Gastrointestinal and Liver Physiology* 2011, 301, G128-G137.

605 [48] Menon, R. M., Barr, W. H., Comparison of ceftibuten transport across Caco-2 cells and rat
606 jejunum mounted on modified Ussing chambers. *Biopharm Drug Dispos* 2003, 24, 299-308.

607 [49] Thwaites, D. T., Anderson, C. M., H⁺-coupled nutrient, micronutrient and drug transporters in
608 the mammalian small intestine. *Experimental physiology* 2007, 92, 603-619.

609 [50] Legen, I., Kristl, A., Factors affecting the microclimate pH of the rat jejunum in ringer
610 bicarbonate buffer. *Biol Pharm Bull* 2003, 26, 886-889.

611 [51] McNeil, N. I., Ling, K. L., Wager, J., Mucosal surface pH of the large intestine of the rat and of
612 normal and inflamed large intestine in man. *Gut* 1987, 28, 707-713.

613 [52] Iwatsubo, T., Miyamoto, Y., Sugiyama, Y., Yuasa, H., *et al.*, Effects of potential damaging agents
614 on the microclimate-pH in the rat jejunum. *J. Pharm. Sci.* 1986, 75, 1162-1165.

615 [53] Coon, S. D., Schwartz, J. H., Rajendran, V. M., Jepeal, L., Singh, S. K., Glucose-dependent
616 insulinotropic polypeptide regulates dipeptide absorption in mouse jejunum. *American Journal of*
617 *Physiology - Gastrointestinal and Liver Physiology* 2013, 305, G678-G684.

618 [54] Rechkemmer, G., Wahl, M., Kuschinsky, W., von Engelhardt, W., pH-microclimate at the luminal
619 surface of the intestinal mucosa of guinea pig and rat. *Pflügers Archiv* 1986, 407, 33-40.

620 [55] Lucas, M. L., Cooper, B. T., Lei, F. H., Johnson, I. T., *et al.*, Acid microclimate in coeliac and
621 Crohn's disease: a model for folate malabsorption. *Gut* 1978, 19, 735-742.

622 [56] Jain, R., Duvvuri, S., Kansara, V., Mandava, N. K., Mitra, A. K., Intestinal absorption of novel-
623 dipeptide prodrugs of saquinavir in rats. *Int. J. Pharm.* 2007, 336, 233-240.

624 [57] Zhang, Q., Liu, Q., Wu, J., Wang, C., *et al.*, PEPT1 involved in the uptake and transepithelial
625 transport of cefditoren in vivo and in vitro. *Eur. J. Pharmacol.* 2009, 612, 9-14.

626 [58] Cang, J., Zhang, J., Wang, C., Liu, Q., *et al.*, Pharmacokinetics and mechanism of intestinal
627 absorption of JBP485 in rats. *Drug metabolism and pharmacokinetics* 2010, 25, 500-507.

628 [59] Knütter, I., Theis, S., Hartrodt, B., Born, I., *et al.*, A novel inhibitor of the mammalian peptide
629 transporter PepT1. *Biochemistry* 2001, *40*, 4454-4458.

630 [60] Yang, B., Smith, D. E., Significance of peptide transporter 1 in the intestinal permeability of
631 Valacyclovir in wild-type and PepT1 knockout mice. *Drug Metab. Disposition* 2013, *41*, 608-614.

632 [61] Matsui, T., Zhu, X. L., Watanabe, K., Tanaka, K., *et al.*, Combined administration of captopril with
633 an antihypertensive Val-Tyr di-peptide to spontaneously hypertensive rats attenuates the blood
634 pressure lowering effect. *Life Sci.* 2006, *79*, 2492-2498.

635 [62] Ten Have, G. A. M., van der Pijl, P. C., Kies, A. K., Deutz, N. E. P., Enhanced lactotripeptide
636 bioavailability by co-ingestion of macronutrients. *PloS one* 2015, *10*, e0130638.

637 [63] Zhu, X.-L., Watanabe, K., Shiraishi, K., Ueki, T., *et al.*, Identification of ACE-inhibitory peptides in
638 salt-free soy sauce that are transportable across caco-2 cell monolayers. *Peptides* 2008, *29*, 338-344.

639 [64] Wessling, S. T., Ross, B. P., Koda, Y., Blanchfield, J. T., Toth, I., Caco-2 cell permeability and
640 stability of two d-glucopyranuronamide conjugates of thyrotropin-releasing hormone. *Biorg. Med.*
641 *Chem.* 2007, *15*, 4946-4950.

642 [65] Ding, L., Zhang, Y., Jiang, Y., Wang, L., *et al.*, Transport of Egg White ACE-Inhibitory Peptide, Gln-
643 lle-Gly-Leu-Phe, in Human Intestinal Caco-2 Cell Monolayers with Cytoprotective Effect. *J. Agric.*
644 *Food Chem.* 2014, *62*, 3177-3182.

645 [66] Vieira, E. F., das Neves, J., Vitorino, R., Dias da Silva, D., *et al.*, Impact of in vitro gastrointestinal
646 digestion and transepithelial transport on antioxidant and ACE-inhibitory activities of Brewers spent
647 yeast autolysate. *J. Agric. Food Chem.* 2016.

648 [67] Sjöberg, Å., Lutz, M., Tannergren, C., Wingolf, C., *et al.*, Comprehensive study on regional human
649 intestinal permeability and prediction of fraction absorbed of drugs using the Ussing chamber
650 technique. *European Journal of Pharmaceutical Sciences* 2013, *48*, 166-180.

651 [68] Koga, K., Kawashima, S., Murakami, M., In vitro and in situ evidence for the contribution of
652 Labrasol® and Gelucire 44/14 on transport of cephalexin and cefoperazone by rat intestine. *Eur J*
653 *Pharm Biopharm* 2002, *54*, 311-318.

654